0013-7227/08/$15.00/0
Printed in U.S.A.

Endocrinology 149(9):4367–4373

doi: 10.1210/en.2008-0018

Thymulin Inhibits Monocrotaline-Induced Pulmonary Hypertension Modulating Interleukin-6 Expression and Suppressing p38 Pathway

Tiago Henriques-Coelho, Sílvia Marta Oliveira, Rute S. Moura, Roberto Roncon-Albuquerque, Jr., Ana Luísa Neves, Mário Santos, Cristina Nogueira-Silva, Filipe La Fuente Carvalho, Ana Brandão-Nogueira, Jorge Correia-Pinto, and Adelino F. Leite-Moreira

Department of Physiology (T.H.-C., S.M.O., R.R.-A., A.L.N., M.S., F.L.F.C., A.B.-N., A.F.L.-M.), Faculty of Medicine, University of Porto, 4200-319 Porto, Portugal; and Life and Health Sciences Research Institute (ICVS) (R.S.M., C.N.-S., J.C.-P.), School of Health Sciences, University of Minho, 4704-553 Braga, Portugal

The pathogenesis of pulmonary hypertension (PH) includes an inflammatory response. Thymulin, a zinc-dependent thymic hormone, has important immunobiological effects by inhibiting various proinflammatory cytokines and chemokines. We investigated morphological and hemodynamic effects of thymulin administration in a rat model of monocrotaline (MCT)-induced PH, as well as the pattern of proinflammatory cytokine gene expression and the intracellular pathways involved. Adult Wistar rats received an injection of MCT (60 mg/kg, sc) or an equal volume of saline. One day after, the animals randomly received during 3 wk an injection of saline, vehicle (zinc plus carboxymethyl cellulose), or thymulin (100 ng/kg, sc, daily). At d 23–25, the animals were anesthetized for hemodynamic recordings, whereas heart and lungs were collected for morphometric and molecular analysis. Thymulin prevented morphological, hemodynamic, and inflammatory cardiopulmonary profile characteristic of MCT-induced PH, whereas part of these effects were also observed in MCT-treated animals injected with the thymulin's vehicle containing zinc. The pulmonary thymulin effect was likely mediated through suppression of p38 pathway. (*Endocrinology* 149: 4367–4373, 2008)

INFLAMMATION SEEMS to play a significant role in the genesis or progression of some forms of pulmonary arterial hypertension (PAH), namely those associated with connective tissue diseases and HIV infection (1, 2). There are several reports that demonstrated the presence of inflammatory cells, including macrophages, polymorphonuclear neutrophils, lymphocytes, and mast cells, in the vicinity of pulmonary vessels and plexiform lesions (3, 4). Elevated levels of the proinflammatory cytokines IL-1 and -6 (5), fractalkine (6), regulated upon activation normal T cell expressed and secreted (7), macrophage inflammatory protein-1a (8), among others, have also been observed in patients with PAH. The role of inflammation in pulmonary hypertension (PH) is further supported by the experimental (9) and clinical (10) improvements observed after steroid treatment or immunosuppressor administration, such as rapamycin (11, 12) or mycophenolate mofetil (13).

Monocrotaline (MCT) and hypoxia models of experimental PH share the involvement of inflammation on its pathophysiology (14, 15). MCT causes endothelial cell damage and mononuclear infiltration into the perivascular regions of arterioles and muscular arteries. By its turn, IL-1 and IL-6, strong proinflammatory cytokines, are excessively produced in animals treated with MCT, and the administration of an IL-1 receptor antagonist reduced PH and right ventricle hypertrophy (9, 16). Further evidence implicating the inflammatory response in the genesis of PH is given by an animal model in which PH was induced by IL-6 administration (17, 18). Multiple studies using serum from patients with PAH have demonstrated increased circulating IL-6 level (5). Moreover, the genome of human herpes virus type 8, which encodes a particularly potent viral IL-6 analog, is associated with PAH in the setting of several diseases, namely HIV/AIDS (19).

Thymulin, also known as "serum thymic factor" (20–23), is a nonapeptide, coupled to ion zinc (24), exclusively secreted by thymic epithelial cells (25, 26). Thymulin enhances an antiinflammatory cytoprotective response and depresses inflammatory cascades (27). Regarding its role in lung diseases, thymulin reduced the cellular inflammatory response and fibrotic changes in an experimental model of lung fibrosis (28). These pulmonary effects were related to an inhibition of the local synthesis of various proinflammatory cytokines and chemokines. Thymulin's beneficial effects in other inflammatory disease models were attributed to

First Published Online May 29, 2008

Abbreviations: AU, Arbitrary unit; Ctrl, control; Ctrl plus S, control rats injected with saline; Ctrl plus T, control rats injected with thymulin; Ctrl plus V, control rats injected with vehicle; dP/dt_{max}, peak rate of right ventricular and left ventricular pressure increase; dP/dt_{min}, peak rate of right ventricular and left ventricular pressure decrease; GAPDH, glyceraldehyde-3-phosphate dehydrogenase; IHC, immunohistochemistry; JNK, c-Jun N-terminal kinase; LV, left ventricular; LVS, left ventricle plus septum; MCT, monocrotaline; MCT plus S, monocrotaline rats injected with saline; MCT plus T, monocrotaline rats injected with thymulin; MCT plus V, monocrotaline rats injected with vehicle; PAH, pulmonary arterial hypertension; PH, pulmonary hypertension; RV, right ventricular; RVP_{max}, peak systolic right ventricular pressure; τ, time constant τ.

***Endocrinology* is published monthly by The Endocrine Society (http://www.endo-society.org), the foremost professional society serving the endocrine community.**

modulation of MAPK family members (29, 30). Thymulin action is strictly dependent on the presence of the metal zinc because it induces the conformational changes within the molecule that are necessary for the full expression of its biological activity (24). Besides being an integral part of this thymic hormone, zinc is essential for many enzymes (31), and plays a role as an antiinflammatory and antioxidant agent (32). The potential role of thymulin in PH has not been studied before. Knowing that MCT induces an early and potent inflammatory response that culminates in severe PH, and that thymulin is an immunoregulatory peptide, the rationale of the present study was to evaluate cardiac and pulmonary effects of thymulin in this experimental model, and exploit the intracellular signaling pathways involved.

Materials and Methods

Study design

Animal experiments were performed according to the Portuguese law for animal welfare and conform to the *Guide for the Care and Use of Laboratory Animals* published by the U.S. National Institutes of Health (National Institutes of Health Publication No. 85-23, revised 1996). Adult male Wistar rats (Charles River, Barcelona, Spain) weighing 180–200 g were housed in groups of five per cage in a controlled environment under a 12-h light, 12-h dark cycle at a room temperature of 22 C, with a free supply of food and water. Rats randomly received a sc injection of MCT (60 mg/kg body weight; Sigma, Barcelona, Spain) or an equal volume of vehicle [control (Ctrl) groups]. One day after, animals from both groups were randomly assigned to receive saline, vehicle, or thymulin, which was injected sc once a day during 3 wk. Vehicle consisted in a solution of carboxymethyl cellulose and zinc without thymulin. Thymulin (100 ng/kg; Sigma) was prepared using carboxymethyl cellulose (0.5%) as a carrier and zinc ($ZnCl_2$; 3.8 μg/ml) as a cofactor (33, 34).

The protocol resulted in six groups: Ctrl rats injected with saline (Ctrl plus S) (n = 6), Ctrl rats injected with vehicle (Ctrl plus V) (n = 6), Ctrl rats injected with thymulin (Ctrl plus T) (n = 6), MCT rats injected with saline (MCT plus S) (n = 8), MCT rats injected with vehicle (MCT plus V) (n = 8), and MCT rats injected with thymulin (MCT plus T) (n = 8). During d 23–25 after MCT or saline injection, the animals were anesthetized and submitted to hemodynamic instrumentation.

Hemodynamic studies

Animals were anesthetized with pentobarbital (60 mg/kg, ip; CEVA), placed over a heating pad, and tracheostomized for mechanical ventilation with room air (Harvard Small Animal Ventilator, Model 683; Harvard Apparatus, Holliston, MA). Anesthesia was maintained with additional bolus of pentobarbital (2 mg/100 g) as needed. Under binocular surgical microscopy (Wild M651.MS-D; Leica, Herbrugg, Switzerland), the right jugular vein was cannulated for fluid administration (prewarmed 0.9% NaCl solution) to compensate for perioperative fluid losses. The heart was exposed through a median sternotomy and the pericardium widely opened. Right and left ventricular (RV and LV, respectively) pressures were measured with a 2F high-fidelity micromanometer (SPR-324; Millar Instruments, Houston, TX) inserted into RV and LV cavities, respectively. After complete instrumentation the animal was allowed to stabilize for 15 min. Hemodynamic recordings were made with ventilation suspended at end expiration. Parameters were converted on line to digital data with a sampling frequency of 1000 Hz. RV and LV pressures were measured at end diastole and peak systole. Peak rates of RV and LV pressure increase (dP/dt_{max}) and pressure decrease (dP/dt_{min}) were measured as well. Relaxation rate was estimated with the time constant τ (τ) by fitting isovolumetric pressure decrease to a monoexponential function.

After hemodynamic evaluation was completed, cardiac arrest was induced by injection of KCl 7.5%. Heart and lungs were excised and weighed. Under binocular magnification (×3.5), the RV free wall was dissected from the left ventricle and septum, and weighed separately. Heart, lung, RV, and left ventricle plus septum (LVS) weights were normalized to body weight, whereas RV weight was normalized to LVS weight. Samples from lung and right ventricle were collected for morphology and molecular analysis.

mRNA quantification

After collection, samples were quickly immersed in RNAlater (QIAGEN, Inc., Valencia, CA) and frozen (−80 C). Total mRNA was extracted through the guanidium-thiocyanate selective silica-gel membrane-binding method (QIAGEN 74124) according to the manufacturer's instructions. Concentration and purity were assayed by spectrophotometry (Eppendorf 6131000.012; Eppendorf International, Hamburg, Germany). Two-step real-time RT-PCR was used to perform relative quantification of mRNA. For each studied mRNA molecule and for each tissue, standard curves were generated from the correlation between the amount of starting total mRNA and PCR threshold cycle (second derivative maximum method) of graded dilutions from a randomly selected tissue sample ($r > 0.97$). For relative quantification of specific mRNA levels, 50 ng total mRNA from each sample underwent two-step real-time RT-PCR. A melt curve analysis of each real-time PCR and 2% agarose gels (0.5 μg/ml ethidium bromide) were performed to exclude primer-dimer formation and assess the purity of the amplification product. Glyceraldehyde-3-phosphate dehydrogenase (GAPDH) mRNA levels were similar in all experimental groups, which enabled the use of this gene as an internal Ctrl. Results of mRNA quantification are expressed in an arbitrary unit (AU) set as the average value of the Ctrl group (1 AU) after normalization for GAPDH. Reverse transcription (20 μl; 10 min at 22 C, 50 min at 50 C, and 10 min at 95 C) was performed in a standard thermocycler (Whatman Biometra 050–901; Goettingen, Germany): 40 U/reaction of reverse transcriptase (Invitrogen 18064-014; Invitrogen Corp., Carlsbad, CA); 20 U/reaction of ribonuclease inhibitor (Promega N2515; Promega Corp., Madison, WI); 30 ng/ml random primers (Invitrogen 48190-011), 0.5 mM nucleotide mix (MBI Fermentas R0192; MBI Fermentas GmbH, St. Leon-Rot, Germany); 1.9 mM $MgCl_2$; and 10 mM dithiothreitol. Of the cDNA yield, 10% was used as a template for real-time PCR (LightCycler II; Roche Diagnostics Corp., Roche Applied Science, Indianapolis, IN) using SYBR green (QIAGEN 204143) according to the manufacturer's instructions. Specific PCR primer pairs for the studied genes were: GAPDH, forward 5′-TGG CCT TCC GTG TTC CTA CCC-3′ and reverse 5′-CCG CCT GCT TCA CCA CCT TCT-3′; IL-6, forward 5′-CCG TTT CTA CCT GGA GTT TG-3′ and reverse 5′-GAA GTT GGG GTA GGA AGG AC-3′; IL-1β, forward 5′-ATG GCA ACT GTC CCT GAA CTC-3′ and reverse 5′-AAT CCT TAA TCT TTT GGG GTC TG-3′; and fractalkine, forward 5′-TGT GTA CTC TGC TGG CGG GTC-3′ and reverse 5′-GTC TCC AGG ATG ATG GCG CGC T-3′.

Immunohistochemistry (IHC) studies

IL-6 immunostainings were performed on formalin-fixed and paraffin-embedded lung. Sections (5 μm) were placed on SuperFrostPlus slides (Menzel Glaser GmbH, Braunschweig, Germany). The primary antibody, a polyclonal goat anti IL-6 (Santa Cruz Biotechnology, Inc., Santa Cruz, CA), was used in a 1:50 dilution. After dewaxing in xylene and rehydration in ethanol, antigen retrieval was achieved by boiling in 10 mM citrate buffer followed by cool down at room temperature. Incubation with the goat ImmunoCruz Staining System (Santa Cruz Biotechnology) was performed according to the manufacturer's instructions. Incubation of the primary antibody occurred at 4 C overnight. Negative Ctrl reactions included omission of the primary antibody. To visualize the peroxidase activities in sections, diaminobenzidine tetrahydrochloride was used. Sections were counterstained with hematoxylin. The slides were observed and photographed with the Olympus BX61 microscope (Olympus, Hamburg, Germany).

Western blot analysis

Lung tissue samples were processed for Western blot analysis. Proteins were obtained according to Kling *et al.* (35). Ten micrograms of protein were loaded onto 10% acrylamide minigels, electrophoresed at 100V at room temperature, and then transferred to Hybond-C Extra (GE Healthcare Life Sciences, Uppsala, Sweden). Blots were probed with polyclonal p38, c-Jun N-terminal kinase (JNK1/2) and p44/42 (ERK1/2), and phospho-p38 (dp-p38), phospho-JNK (dp-JNK1/2), and phospho-

TABLE 1. Morphometric parameters

	Ctrl groups			MCT groups			*P* value
	Saline	Vehicle	Thymulin	Saline	Vehicle	Thymulin	
Body wt (g)	287 ± 9	293 ± 4	288 ± 7	269 ± 6	278 ± 9	279 ± 10	
Heart wt/body wt (g/kg)	3.01 ± 0.11	2.70 ± 0.06	2.95 ± 0.06	3.83 ± 0.17[a]	2.89 ± 0.09[b]	2.99 ± 0.11[b]	[c]
RV wt/body wt (g/kg)	0.55 ± 0.02	0.62 ± 0.03	0.63 ± 0.03	1.15 ± 0.06[a]	0.83 ± 0.08[b,d]	0.67 ± 0.06[b]	[c]
RV/LVS	0.25 ± 0.03	0.33 ± 0.01	0.30 ± 0.03	0.501 ± 0.02[a]	0.44 ± 0.05[d]	0.34 ± 0.02[b,e]	
Lung wt/body wt (g/kg)	4.66 ± 0.16	4.42 ± 0.15	4.45 ± 0.16	12.44 ± 1.01[a]	7.95 ± 1.05[b,d]	6.63 ± 0.39[b]	[c]

Data are presented as mean ± SEM. RV, Right ventricle; wt, weight.
[a] $P < 0.05$ *vs.* Ctrl plus S.
[b] $P < 0.05$ *vs.* MCT plus S.
[c] Interaction.
[d] $P < 0.05$ *vs.* Ctrl plus V.
[e] $P < 0.05$ *vs.* MCT plus V.

p44/42 (dp-ERK1/2), antibodies (Cell Signaling Technology, Inc., Danvers, MA) according to the manufacturer's instructions. For loading Ctrl, blots were probed with β-tubulin rabbit polyclonal antibody (1:100,000) (Abcam plc, Cambridge, UK). Afterwards, blots were incubated with a secondary horseradish peroxidase conjugate (1:2000) (Cell Signaling Technology). Membranes probed simultaneously with p38 and JNK, as well as dp-p38 and dp-JNK, were stripped [62.5 mM Tris-HCl (pH 6.7), 2% sodium dodecyl sulfate, and 100 mM 2-mercaptoethanol] for 30 min at 50 C and then incubated with β-tubulin. Membranes were developed with Super Signal West Femto Substrate (Pierce, Rockford, IL) and ChemiDoc XRS System (Bio-Rad Laboratories, Inc., Hercules, CA). Quantitative analysis was performed with Quantity One 4.6.5 1-D Analysis Software (Bio-Rad Laboratories).

Statistical analysis

The results were presented as mean ± SEM and were compared using two-way ANOVA. When treatments were significantly different, the Holm-Sidak test was selected to perform pairwise multiple comparisons. Statistical significance was set at $P < 0.05$.

Results

Morphometric data

Cardiac and lung morphometric data are summarized in Table 1. Administration of vehicle or thymulin to Ctrl animals did not affect any of the studied morphometric parameters.

MCT induced a statistically significant increase in heart and lung weights, when compared with the Ctrl plus S group. PH induced by MCT resulted in RV hypertrophy without affecting LV weight. Administration of both vehicle and thymulin significantly decreased morphometric changes induced by MCT, although the beneficial effects were more pronounced in thymulin-treated animals.

Biventricular hemodynamics

Hemodynamic data are summarized in Table 2. In Ctrl groups, neither vehicle nor thymulin modified the studied hemodynamic parameters. MCT induced a significant increase in peak systolic RV pressure (RVP_{max}), a parameter used to estimate PH, as well as in RV dP/dt_{max}, an index of RV contractility. Regarding RV diastolic function, relaxation rate as estimated by the τ was prolonged in MCT-treated animals. MCT-treated animals that received vehicle presented less PH when compared with the MCT plus S group, whereas MCT-treated animals that received thymulin did not demonstrate any hemodynamic evidence of PH. Indeed, there was no increase in RVP_{max} or changes in dP/dt_{max}. Concerning RV diastolic function, τ was not different from Ctrl animals.

With regard to LV function, the MCT plus S group presented, when compared with the Ctrl plus S group, lower systolic and end-diastolic pressures, and smaller peak rates

TABLE 2. Biventricular hemodynamic parameters

	Ctrl groups			MCT groups			*P* value
	Saline	Vehicle	Thymulin	Saline	Vehicle	Thymulin	
Right ventricle							
RVP_{max} (mm Hg)	25.5 ± 2.1	25.7 ± 0.7	24.9 ± 1.1	46.6 ± 1.9[a]	41.9 ± 3.1[b,c]	26.8 ± 3.6[c,d]	[e]
RV-EDP (mm Hg)	1.9 ± 0.5	1.9 ± 0.6	1.6 ± 0.6	1.4 ± 0.4	1.1 ± 0.2	0.8 ± 0.3	
dP/dt_{max} (mm Hg/sec)	1192 ± 80	1012 ± 116	1148 ± 51	1679 ± 149[a]	1249 ± 123[c]	1220 ± 82[c]	
dP/dt_{min} (mm Hg/sec)	−973 ± 85	−912 ± 69	−900 ± 97	−1218 ± 90	−1201 ± 141	−960 ± 111	
τ (msec)	12 ± 1	12 ± 2	14 ± 1	27 ± 1[a]	28 ± 2[b]	13 ± 1[c,d]	[e]
Left ventricle							
LVP_{max} (mm Hg)	104.9 ± 6.8	104.3 ± 13.2	107.6 ± 5.2	68.1 ± 8.5[a]	76.7 ± 9.8[b]	94.7 ± 7.3[c]	
LV-EDP (mm Hg)	3.7 ± 0.3	3.5 ± 0.4	3.6 ± 0.6	1.7 ± 0.4[a]	3.1 ± 0.4	2.6 ± 0.3	
dP/dt_{max} (mm Hg/sec)	5711 ± 589	5654 ± 987	6162 ± 418	3519 ± 338[a]	4274 ± 296	5510 ± 460	
dP/dt_{min} (mm Hg/sec)	−3349 ± 404	−3170 ± 624	−3372 ± 249	−1950 ± 233[a]	−2000 ± 318[b]	−3460 ± 399[c,d]	
τ (msec)	21 ± 1	18 ± 1	20 ± 1	22 ± 1	22 ± 1	19 ± 1	

Data are presented as mean ± SEM. LVP_{max}, LV peak systolic pressure; RV-EDP and LV-EDP, RV and LV end-diastolic pressures, respectively.
[a] $P < 0.05$ *vs.* Ctrl plus S.
[b] $P < 0.05$ *vs.* Ctrl plus V.
[c] $P < 0.05$ *vs.* MCT plus S.
[d] $P < 0.05$ *vs.* MCT plus V.
[e] Interaction.

of pressure increase and decrease. The MCT plus V group kept a significant decrease in peak systolic LV pressure. In MCT-treated animals that received thymulin, no hemodynamic disturbances were observed in the left ventricle. There were no statistically significant differences between this group and Ctrl plus T animals. The τ did not differ among the groups.

Pro-inflammatory cytokines

Pro-inflammatory cytokines IL-1β, IL-6, and fractalkine mRNA levels were measured in lung and RV myocardial samples by real-time PCR (Fig. 1).

In lung, MCT treatment induced a significant increase in IL-6 mRNA, without changing the other analyzed cytokines (Fig. 1, *left panel*). In MCT-treated animals, both vehicle and thymulin induced a statistically significant decrease in IL-6 mRNA expression.

IHC studies were performed to identify the pattern of cellular expression of IL-6 in the lung. In Ctrl animals (Fig. 2, A–C), IL-6 is mainly expressed in smooth muscle cells both in arterial and bronchial walls, and weakly in bronchial epithelial cells and vascular endothelium. In MCT-treated animals (Fig. 2, D–F), a similar pattern was observed. However, the intensity of this staining seems to be increased in the MCT plus S group. In contrast to the Ctrl group, the MCT groups presented an infiltration of mononuclear inflammatory cells expressing IL-6 protein.

In the right ventricle, MCT administration induced a strong up-regulated IL-6 expression, and a slight increase in IL-1β and fractalkine mRNA levels (Fig. 1, *right panel*). In MCT-treated animals, both vehicle and thymulin normalized IL-6 mRNA expression.

MAPK signaling pathway

Pulmonary protein levels of p38, JNK1/2, and ERK1/2 (both unphosphorylated and phosphorylated forms) were analyzed by Western blot and quantified by densitometric analysis (Fig. 3).

In Ctrl animals both vehicle and thymulin groups exhibited an increase of phosphorylated p38 protein levels. In comparison with Ctrl animals treated with saline, MCT animals injected with saline revealed an enhancement of p38 and JNK1/2 phosphorylation, whereas no significant effect was observed in ERK pathway. In MCT-treated animals, both vehicle and thymulin reduced JNK phosphorylation. Thymulin induced a specific and strong inhibition of p38 pathway, whereas vehicle did not modify this MAPK pathway.

Discussion

In the present study, we demonstrated that thymulin prevented morphological, hemodynamic, and inflammatory cardiopulmonary profile characteristics of MCT-induced PH, whereas part of these effects were also observed in MCT-treated animals injected with the thymulin's vehicle containing zinc. The pulmonary thymulin effect was likely mediated through suppression of p38 pathway.

The pathogenesis of PH involves vasoconstriction, pulmonary vascular remodeling, *in situ* thrombosis, and inflammation. The inflammatory hypothesis of PH is supported by both experimental and human studies (3–8). PH induced by MCT is an experimental model with some similarities with human PAH, such as hemodynamic repercussions, histological changes, and high mortality (36). On the other hand, it diverges from human PAH in the precocious loss of endothelial barrier and in the inflammatory adventitial proliferation (15).

Inflammation is a main feature of the MCT model, as demonstrated by early inflammatory cells recruitment (37) and cytokine activation (9). To clarify the underlying mechanisms of MCT-induced PH, inflammatory cytokine expression and MAPK activation were examined. We observed an

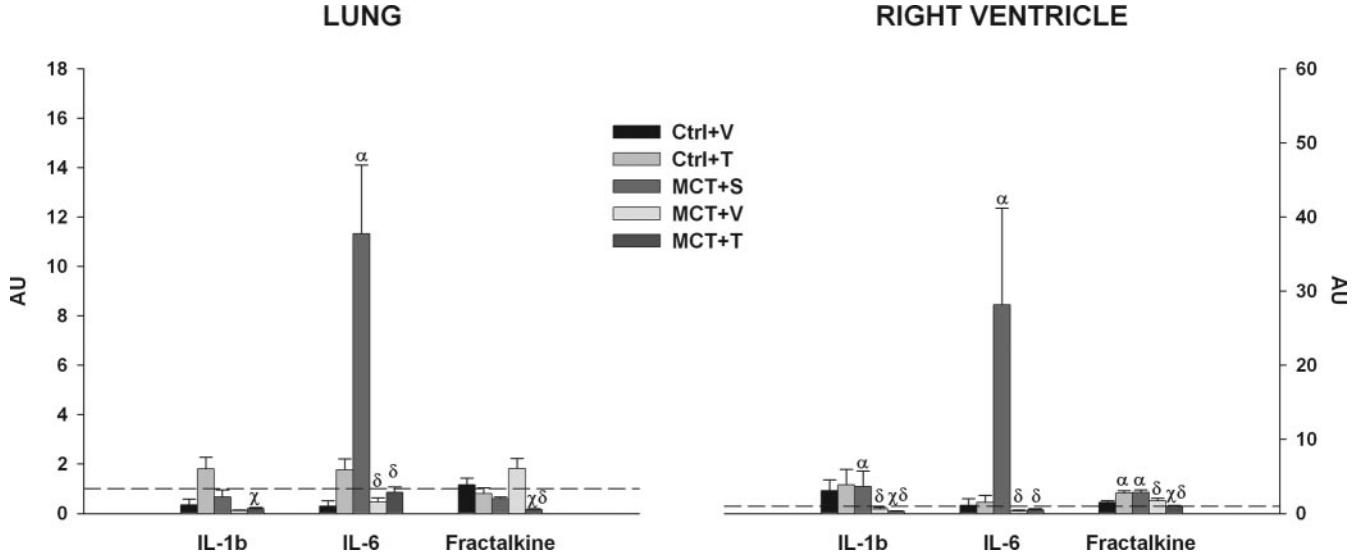

FIG. 1. Lung and right ventricle IL-1β, IL-6, and fractalkine mRNA levels, normalized for GAPDH (housekeeping gene) and expressed as AUs, in the six studied groups: Ctrl plus S, Ctrl plus V, Ctrl plus T, MCT plus S, MCT plus V, and MCT plus T. $P < 0.05$: $^{\alpha,}$ *vs.* Ctrl plus S; $^{\chi,}$ *vs.* Ctrl plus T; $^{\delta,}$ *vs.* MCT plus S.

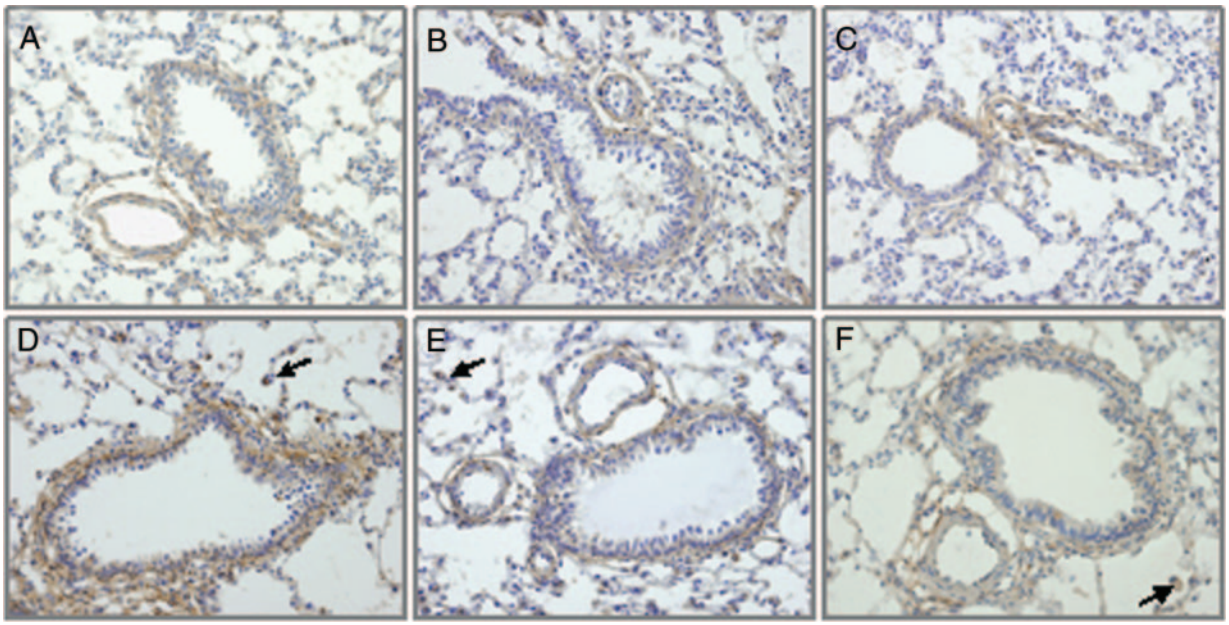

FIG. 2. Pulmonary IL-6 protein expression in different experimental groups by IHC. A, Ctrl plus S animals. B, Ctrl plus V animals. C, Ctrl plus T animals. D, MCT plus S animals. E, MCT plus V animals. F, MCT plus T animals. All images are at the same magnification (×200). *Arrows* displayed IL-6 positive inflammatory cells.

increase in IL-6 gene expression not only in the lungs but also in the right ventricle in the fourth week after MCT injection. These findings confirm previous results from Bhargava *et al.* (9) that demonstrated elevated levels of IL-6 at 48 h, 1 and 2 wk after MCT injection. We also evaluated IL-1β and fractalkine, other cytokines typically involved in human PH pathophysiology, but in our study MCT did not increase these cytokines in the lung tissue and had a very mild effect in the myocardium.

MAPKs are important mediators of signal transduction processes, and are activated in a variety of physiological and pathological conditions. Lu *et al.* (38) found an increase in p38 MAPK activity in lungs from rats treated with MCT and prevented the progression to PH through the administration of a selective p38 inhibitor. On other hand, Morty *et al.* (39) only observed a slight reduction in ERK1/2 phosphorylation, and no change in p38 MAPK phosphorylation. In our study we demonstrated an increase in both p38 and JNK phosphorylation in the MCT-treated animals, confirming the involvement MAPK pathways in PH pathophysiology. On the other hand, zinc exposure has activated several MAPKs in airway epithelial cells (40, 41). Levels of MAPK phosphorylation are regulated in opposite directions by MAPK kinases and phosphatases (42), and zinc seems to act through inhibition MAPK phosphatase activity (40). In fact, our data also suggest that in Ctrl animals, zinc has an important role in modulating MAPK, namely p38 phosphorylation. However, in MCT-treated animals, zinc exposure did not change the pattern of p38 activation, whereas thymulin treatment resulted in a significant decrease in p38 phosphorylation.

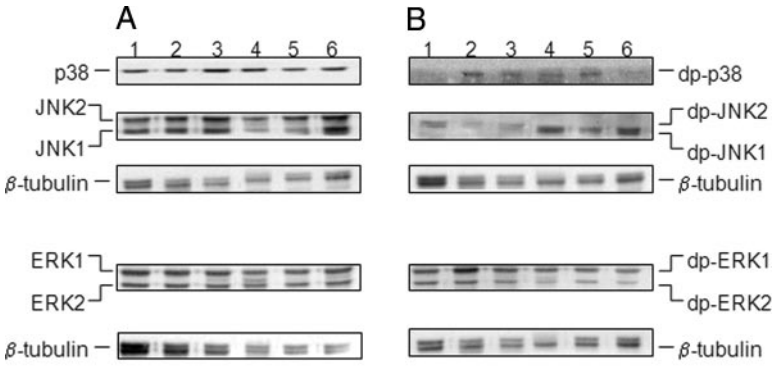

C

	1. Ctrl+S	2. Ctrl+V	3. Ctrl+T	4. MCT+S	5. MCT+V	6. MCT+T
dp-p38	1	3.5	3.3	2.0	3.1	0.7
dp-JNK1/2	1	0.8	2.3	8.2	4.2	5.8
dp-ERK1/2	1	2.4	1.4	1.1	1.8	0.6

FIG. 3. MAPK activities at pulmonary level in Ctrl plus S animals (1), Ctrl plus V animals (2), Ctrl plus T animals (3), MCT plus S animals (4), MCT plus V animals (5), and MCT plus T animals (6). Western blot analysis of MAPK with antibodies to p38, ERK1/2, and JNK1/2 (A), and to diphosphorylated forms of p38 (dp-p38), ERK1/2 (dp-ERK1/2), and SAPK/JNK (dp-JNK1/2) (B). Ctrl loading was performed using β-tubulin (55 kDa). ERK1 and 2 correspond to 44 and 42 kDa, respectively. JNK1 and 2 correspond to 46 and 54 kDa, respectively. p38 corresponds to 38 kDa. Quantitative analysis for dp-p38, dp-ERK1/2, and dp-JNK1/2 are presented as AUs in the six studied groups (C).

Thymulin has a potent immunomodulator effect, in addition to its action as a thymic hormone. Previous reports have shown that thymulin prevents bleomycin-induced pulmonary fibrosis (28), alloxan- and streptozotocin-induced diabetes (43), myocarditis caused by the encephalomyocarditis virus (44), and cisplatin- (29) and cephaloridine-induced nephrotoxicity (30). In the setting of PH, our data revealed that thymulin administration prevented biventricular hemodynamic changes typically found in the MCT model. Part of these effects had been also observed in animals treated with vehicle containing zinc. These beneficial effects could be partially explained by IL-6 suppression at pulmonary and myocardium levels, reinforcing the pivotal role of IL-6 in PH pathogenesis. In fact, delivery of recombinant IL-6 protein reproduced the main hemodynamic and histological features of PH in a rat model (17), and inhibition of IL-6 with dexamethasone (9) or serotonin antagonist (18) prevented the development of PH. IL-6 exerts its effects by activation of the janus kinase/signal transducers and activators of transcription-signaling pathway and induction of the MAPK cascade (45). *In vitro*, IL-6 stimulated lung branching through activation of p38-MAPK intracellular pathway (46). Recently, Hagen *et al*. (47) demonstrated the presence of a negative feedback loop between IL-6 and the bone morphogenetic protein pathway mediated through p38 MAPK activity, and proposed that IL-6 activation can be the inflammatory "second hit" in patients with familial PAH with bone morphogenetic protein receptor 2 mutations.

In conclusion, we demonstrated that thymulin inhibited the development of PH in the MCT model. This effect could be related to the inhibition of proinflammatory IL-6 expression and suppression of p38 phosphorylation.

Acknowledgments

We thank Antónia Teles for her invaluable technical assistance in this study.

Received January 4, 2008. Accepted May 21, 2008.

Address all correspondence and requests for reprints to: Professor Adelino F. Leite-Moreira, Department of Physiology, Faculty of Medicine, Alameda Professor Hernâni Monteiro, 4200-319 Porto, Portugal. E-mail: amoreira@med.up.pt.

This work was supported by grants from the Portuguese Foundation for Science and Technology (No. POCI/SAVFCF/60803/2004; POCTI/SAV-MMO/61547/2004 and PTDC/SAV-FCF/65793/2006) through Cardiovascular R&D Unit (FCT No. 51/94). R.S.M. was supported by Fundação para a Ciência e a Tecnologia (reference SFRH/BPD/15408/2005).

Disclosure Statement: The authors have nothing to disclose.

References

1. **Simonneau G, Galie N, Rubin LJ, Langleben D, Seeger W, Domenighetti G, Gibbs S, Lebrec D, Speich R, Beghetti M, Rich S, Fishman A** 2004 Clinical classification of pulmonary hypertension. J Am Coll Cardiol 43(Suppl S):5S–12S
2. **Galie N, Torbicki A, Barst R, Dartevelle P, Haworth S, Higenbottam T, Olschewski H, Peacock A, Pietra G, Rubin LJ, Simonneau G, Priori SG, Garcia MA, Blanc JJ, Budaj A, Cowie M, Dean V, Deckers J, Burgos EF, Lekakis J, Lindahl B, Mazzotta G, McGregor K, Morais J, Oto A, Smiseth OA, Barbera JA, Gibbs S, Hoeper M, Humbert M, Naeije R, Pepke-Zaba J, Task Force** 2004 Guidelines on diagnosis and treatment of pulmonary arterial hypertension. The Task Force on Diagnosis and Treatment of Pulmonary Arterial Hypertension of the European Society of Cardiology. Eur Heart J 25:2243–2278
3. **Tuder RM, Groves B, Badesch DB, Voelkel NF** 1994 Exuberant endothelial cell growth and elements of inflammation are present in plexiform lesions of pulmonary hypertension. Am J Pathol 144:275–285
4. **Cool CD, Kennedy D, Voelkel NF, Tuder RM** 1997 Pathogenesis and evolution of plexiform lesions in pulmonary hypertension associated with scleroderma and human immunodeficiency virus infection. Hum Pathol 28:434–442
5. **Humbert M, Monti G, Brenot F, Sitbon O, Portier A, Grangeot-Keros L, Duroux P, Galanaud P, Simonneau G, Emilie D** 1995 Increased interleukin-1 and interleukin-6 serum concentrations in severe primary pulmonary hypertension. Am J Respir Crit Care Med 151:1628–1631
6. **Balabanian K, Foussat A, Dorfmuller P, Durand-Gasselin I, Capel F, Bouchet-Delbos L, Portier A, Marfaing-Koka A, Krzysiek R, Rimaniol AC, Simonneau G, Emilie D, Humbert M** 2002 CX(3)C chemokine fractalkine in pulmonary arterial hypertension. Am J Respir Crit Care Med 165:1419–1425
7. **Dorfmuller P, Zarka V, Durand-Gasselin I, Monti G, Balabanian K, Garcia G, Capron F, Coulomb-Lhermine A, Marfaing-Koka A, Simonneau G, Emilie D, Humbert M** 2002 Chemokine RANTES in severe pulmonary arterial hypertension. Am J Respir Crit Care Med 165:534–539
8. **Fartoukh M, Emilie D, Le Gall C, Monti G, Simonneau G, Humbert M** 1998 Chemokine macrophage inflammatory protein-1α mRNA expression in lung biopsy specimens of primary pulmonary hypertension. Chest 114(Suppl): 50S–51S
9. **Bhargava A, Kumar A, Yuan N, Gewitz MH, Mathew R** 1999 Monocrotaline induces interleukin-6 mRNA expression in rat lungs. Heart Dis 1:126–132
10. **Karmochkine M, Wechsler B, Godeau P, Brenot F, Jagot JL, Simonneau G** 1996 Improvement of severe pulmonary hypertension in a patient with SLE. Ann Rheum Dis 55:561–562
11. **Nishimura T, Faul JL, Berry GJ, Veve I, Pearl RG, Kao PN** 2001 40-O-(2-hydroxyethyl)-rapamycin attenuates pulmonary arterial hypertension and neointimal formation in rats. Am J Respir Crit Care Med 163:498–502
12. **Paddenberg R, Stieger P, von Lilien AL, Faulhammer P, Goldenberg A, Tillmanns HH, Kummer W, Braun-Dullaeus RC** 2007 Rapamycin attenuates hypoxia-induced pulmonary vascular remodeling and right ventricular hypertrophy in mice. Respir Res 8:15
13. **Suzuki C, Takahashi M, Morimoto H, Izawa A, Ise H, Hongo M, Hoshikawa Y, Ito T, Miyashita H, Kobayashi E, Shimada K, Ikeda U** 2006 Mycophenolate mofetil attenuates pulmonary arterial hypertension in rats. Biochem Biophys Res Commun 349:781–788
14. **Dorfmuller P, Perros F, Balabanian K, Humbert M** 2003 Inflammation in pulmonary arterial hypertension. Eur Respir J 22:358–363
15. **Naeije R, Dewachter L** 2007 [Animal models of pulmonary arterial hypertension.] Rev Mal Respir 24(4 Pt 1):481–496 (French)
16. **Voelkel NF, Tuder RM, Bridges J, Arend WP** 1994 Interleukin-1 receptor antagonist treatment reduces pulmonary hypertension generated in rats by monocrotaline. Am J Respir Cell Mol Biol 11:664–675
17. **Miyata M, Sakuma F, Yoshimura A, Ishikawa H, Nishimaki T, Kasukawa R** 1995 Pulmonary hypertension in rats. 2. Role of interleukin-6. Int Arch Allergy Immunol 108:287–291
18. **Miyata M, Ito M, Sasajima T, Ohira H, Kasukawa R** 2001 Effect of a serotonin receptor antagonist on interleukin-6-induced pulmonary hypertension in rats. Chest 119:554–561
19. **Deng H, Song MJ, Chu JT, Sun R** 2002 Transcriptional regulation of the interleukin-6 gene of human herpesvirus 8 (Kaposi's sarcoma-associated herpesvirus). J Virol 76:8252–8264
20. **Bach JF, Dardenne M, Pleau JM, Rosa J** 1976 [Biochemical characterization of a circulating thymic factor.] C R Acad Sci Hebd Seances Acad Sci D 283:1605–1607 (French)
21. **Dardenne M, Pleau JM, Man NK, Bach JF** 1977 Structural study of circulating thymic factor: a peptide isolated from pig serum. I. Isolation and purification. J Biol Chem 252:8040–8044
22. **Pleau JM, Dardenne M, Blouquit Y, Bach JF** 1977 Structural study of circulating thymic factor: a peptide isolated from pig serum. II. Amino acid sequence. J Biol Chem 252:8045–8047
23. **Bach JF, Dardenne M, Pleau JM, Bach MA** 1975 Isolation, biochemical characteristics, and biological activity of a circulating thymic hormone in the mouse and in the human. Ann NY Acad Sci 249:186–210
24. **Dardenne M, Pleau JM, Nabarra B, Lefrancier P, Derrien M, Choay J, Bach JF** 1982 Contribution of zinc and other metals to the biological activity of the serum thymic factor. Proc Natl Acad Sci USA 79:5370–5373
25. **Savino W, Huang PC, Corrigan A, Berrih S, Dardenne M** 1984 Thymic hormone-containing cells. V. Immunohistological detection of metallothionein within the cells bearing thymulin (a zinc-containing hormone) in human and mouse thymuses. J Histochem Cytochem 32:942–946
26. **Dardenne M, Savino W, Gagnerault MC, Itoh T, Bach JF** 1989 Neuroendocrine control of thymic hormonal production. I. Prolactin stimulates *in vivo* and *in vitro* the production of thymulin by human and murine thymic epithelial cells. Endocrinology 125:3–12
27. **Haddad JJ, Land SC, Saade NE, Safieh-Garabedian B** 2000 Immunomodulatory potential of thymulin-Zn(2+) in the alveolar epithelium: amelioration of endotoxin-induced cytokine release and partial amplification of a cytoprotective IL-10-sensitive pathway. Biochem Biophys Res Commun 274:500–505
28. **Yara S, Kawakami K, Kudeken N, Tohyama M, Teruya K, Chinen T, Awaya A, Saito A** 2001 FTS reduces bleomycin-induced cytokine and chemokine

production and inhibits pulmonary fibrosis in mice. Clin Exp Immunol 124:77–85
29. **Kohda Y, Kawai Y, Iwamoto N, Matsunaga Y, Aiga H, Awaya A, Gemba M** 2005 Serum thymic factor, FTS, attenuates cisplatin nephrotoxicity by suppressing cisplatin-induced ERK activation. Biochem Pharmacol 70:1408–1416
30. **Kohda Y, Matsunaga Y, Yonogi K, Kawai Y, Awaya A, Gemba M** 2005 Protective effect of serum thymic factor, FTS, on cephaloridine-induced nephrotoxicity in rats. Biol Pharm Bull 28:2087–2091
31. **Varin A, Larbi A, Dedoussis GV, Kanoni S, Jajte J, Rink L, Monti D, Malavolta M, Marcellini F, Mocchegiani E, Herbein G, Fulop Jr T** 2008 In vitro and in vivo effects of zinc on cytokine signalling in human T cells. Exp Gerontol 43:472–482
32. **Prasad AS** 2008 Clinical, immunological, anti-inflammatory and antioxidant roles of zinc. Exp Gerontol 43:370–377
33. **Oliver MA, Marsh JA** 2003 In vivo thymulin treatments enhance avian lung natural killer cell cytotoxicity in response to infectious bronchitis virus. Int Immunopharmacol 3:107–113
34. **Orringer DA, Staeheli P, Marsh JA** 2002 The effects of thymulin on macrophage responsiveness to interferon-γ. Dev Comp Immunol 26:95–102
35. **Kling DE, Lorenzo HK, Trbovich AM, Kinane TB, Donahoe PK, Schnitzer JJ** 2002 MEK-1/2 inhibition reduces branching morphogenesis and causes mesenchymal cell apoptosis in fetal rat lungs. Am J Physiol Lung Cell Mol Physiol 282:L370–L378
36. **Henriques-Coelho T, Correia-Pinto J, Roncon-Albuquerque Jr R, Baptista MJ, Lourenco AP, Oliveira SM, Brandao-Nogueira A, Teles A, Fortunato JM, Leite-Moreira AF** 2004 Endogenous production of ghrelin and beneficial effects of its exogenous administration in monocrotaline-induced pulmonary hypertension. Am J Physiol Heart Circ Physiol 287:H2885–H2890
37. **Roth RA, Reindel JF** 1991 Lung vascular injury from monocrotaline pyrrole, a putative hepatic metabolite. Adv Exp Med Biol 283:477–487
38. **Lu J, Shimpo H, Shimamoto A, Chong AJ, Hampton CR, Spring DJ, Yada M, Takao M, Onoda K, Yada I, Pohlman TH, Verrier ED** 2004 Specific inhibition of p38 mitogen-activated protein kinase with FR167653 attenuates vascular proliferation in monocrotaline-induced pulmonary hypertension in rats. J Thorac Cardiovasc Surg 128:850–859
39. **Morty RE, Nejman B, Kwapiszewska G, Hecker M, Zakrzewicz A, Kouri FM, Peters DM, Dumitrascu R, Seeger W, Knaus P, Schermuly RT, Eickelberg O** 2007 Dysregulated bone morphogenetic protein signaling in monocrotaline-induced pulmonary arterial hypertension. Arterioscler Thromb Vasc Biol 27:1072–1078
40. **Kim YM, Reed W, Wu W, Bromberg PA, Graves LM, Samet JM** 2006 Zn2+-induced IL-8 expression involves AP-1, JNK, and ERK activities in human airway epithelial cells. Am J Physiol Lung Cell Mol Physiol 290:L1028–L1035
41. **Samet JM, Graves LM, Quay J, Dailey LA, Devlin RB, Ghio AJ, Wu W, Bromberg PA, Reed W** 1998 Activation of MAPKs in human bronchial epithelial cells exposed to metals. Am J Physiol 275(3 Pt 1):L551–L558
42. **Farooq A, Zhou MM** 2004 Structure and regulation of MAPK phosphatases. Cell Signal 16:769–779
43. **Yamanouchi T, Moromizato H, Kojima S, Shinohara T, Sekino N, Minoda S, Miyashita H, Akaoka I** 1994 Prevention of diabetes by thymic hormone in alloxan-treated rats. Eur J Pharmacol 257:39–46
44. **Mizutani M, El-Fotoh M, Mori M, Ono K, Doi K, Awaya A, Matsumoto Y, Matsumoto Y, Onodera T** 1996 In vivo administration of serum thymic factor (FTS) prevents EMC-D virus-induced diabetes and myocarditis in BALB/cAJcl mice. Arch Virol 141:73–83
45. **Heinrich PC, Behrmann I, Haan S, Hermanns HM, Muller-Newen G, Schaper F** 2003 Principles of interleukin (IL)-6-type cytokine signalling and its regulation. Biochem J 374(Pt 1):1–20
46. **Nogueira-Silva C, Santos M, Baptista MJ, Moura RS, Correia-Pinto J** 2006 IL-6 is constitutively expressed during lung morphogenesis and enhances fetal lung explant branching. Pediatr Res 60:530–536
47. **Hagen M, Fagan K, Steudel W, Carr M, Lane K, Rodman DM, West J** 2007 Interaction of interleukin-6 and the BMP pathway in pulmonary smooth muscle. Am J Physiol Lung Cell Mol Physiol 292:L1473–L1479

***Endocrinology* is published monthly by The Endocrine Society (http://www.endo-society.org), the foremost professional society serving the endocrine community.**